STABILITY ANALYSIS FOR THE IMMERSED FIBER PROBLEM *

JOHN M. STOCKIE† AND BRIAN T. R. WETTON†

Abstract. A linear stability analysis is performed on a two-dimensional version of the "immersed fiber problem", formulated by C. Peskin to model the flow of fluid in the presence of a mesh of moving, elastic fibers. The purpose of the analysis is to isolate the modes in the solution which are associated with the fiber, and thereby determine the effect of the presence of a fiber on the fluid. The results are used not only to make conclusions about the stability of the problem, but also to suggest guidelines for developing numerical methods for flows with immersed fibers.

Key words. immersed boundary problem, linear stability

AMS subject classifications. (primary) 35B30, (secondary) 76D05, 65M12

1. Introduction. This paper is concerned with the stability of incompressible, viscous fluid flows in the presence of moving, elastic fibers. A mesh of such fibers was used by Peskin in [7] to model muscle tissue immersed in blood, leading to the development of a numerical scheme for computing the flow of blood within the heart. His "Immersed Boundary Method" facilitated realistic computations of flows with complex, elastic structures suspended in fluid. The method was extended to a three-dimensional model of the heart in [8] and has also been applied to various other physical problems involving the motion of immersed elastic fibers (such as aquatic animal locomotion in [4] and fluid flow in the inner ear in [2]). Recently, some theoretical work has been performed on the numerical methods used to compute problems with immersed fibers; for example, the work of Beyer & LeVeque [1], Tu & Peskin [10] and LeVeque & Li [5]. However, to our knowledge, no analysis has been performed on the equations of motion themselves.

The basic idea in this paper is to examine the stability of the underlying differential equations for a simplified two-dimensional model of the immersed boundary problem. By performing a linear analysis, we concentrate on the modes associated with the fiber and thereby determine the stability characteristics of flows with immersed fibers. Based on these analytical results, conclusions will be drawn regarding not only the structure of the problem and hence the type of behaviour to expect in computed solutions, but also the numerical methods which should be employed for flows containing immersed fibers.

2. The Immersed Fiber Problem. To simplify the analysis, we will consider a two-dimensional analogue of the three-dimensional problem posed by Peskin & McQueen in [8] for the purpose of computing the flow of blood in the heart. First, define a fluid domain $\Omega \subset I\!R^2$ within which is suspended a single, isolated fiber Γ (refer to Figure 1). The fiber position is given by $\boldsymbol{x} = (x, y) = \boldsymbol{X}(s, t)$, where s is the arclength along the fiber in some reference configuration. The fiber is assumed to have zero mass and volume, and to adhere to adjacent fluid particles. Consequently, the fluid and fiber may be considered as a composite material whose motion is described by the single velocity field $\boldsymbol{u} = \boldsymbol{u}(\boldsymbol{x}, t) = (u(\boldsymbol{x}, t), v(\boldsymbol{x}, t))$, with corresponding pressure $p(\boldsymbol{x}, t)$. The fluid is taken to be Newtonian and incompressible, with constant density and kinematic viscosity, ν; hence, the motion of the fluid-fiber composite is governed

* Both authors were supported by grants from NSERC Canada.

† Institute of Applied Mathematics, University of British Columbia, Vancouver, BC, Canada

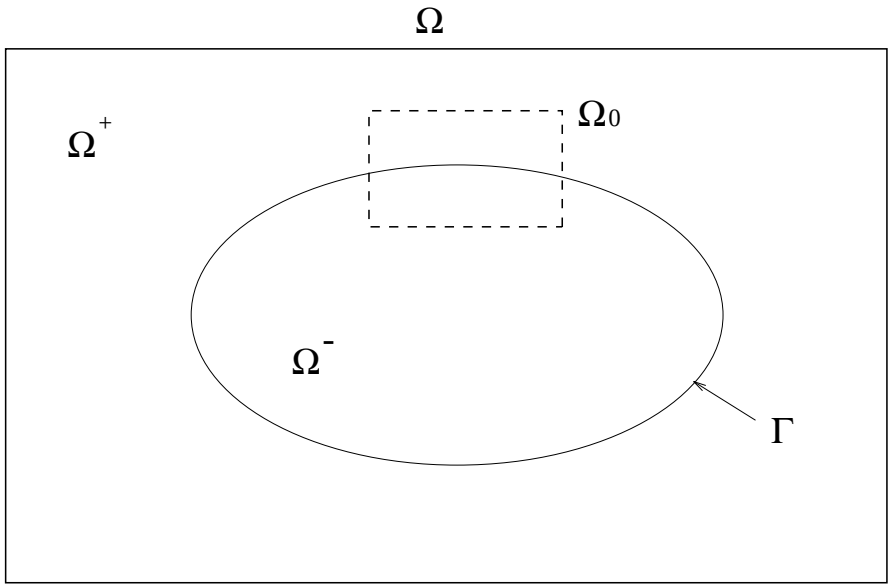

FIG. 1. *A two-dimensional model of the heart: the fluid domain, Ω, which is divided into two parts, Ω^+ and Ω^-, by an isolated fiber Γ immersed in the fluid. The subdomain Ω_0 (delimited by dashed lines) is the region considered in the linearized version of the immersed fiber problem.*

by the Navier-Stokes equations,

$$\boldsymbol{u}_t = -\boldsymbol{u}\cdot\nabla\boldsymbol{u} + \nu\Delta\boldsymbol{u} - \nabla p + \boldsymbol{F}, \tag{1}$$

$$\nabla\cdot\boldsymbol{u} = 0, \tag{2}$$

where both pressure and force have been normalized by the constant density. The requirement that the fiber move at the local fluid velocity is equivalent to

$$\frac{\partial \boldsymbol{X}}{\partial t} = \boldsymbol{u}(\boldsymbol{X}(s,t),t). \tag{3}$$

One more element is needed to close the system, namely an expression for the force $\boldsymbol{F}$ in (1). External forces are assumed to be negligible so that $\boldsymbol{F}$ must arise solely from elastic forces exerted by the fiber on neighbouring fluid particles. Let $T(s,t)$ be the force of tension in the fiber and assume that T is of the form

$$T = \sigma\left(\left|\frac{\partial \boldsymbol{X}}{\partial s}\right|\right). \tag{4}$$

Notice that $|d\boldsymbol{X}| = |\partial\boldsymbol{X}/\partial s|\cdot|ds|$, where $|d\boldsymbol{X}|$ is the distance between two points on the fiber, and $|ds|$ is the distance between the same two points in the reference configuration; hence, $|\partial\boldsymbol{X}/\partial s|$ is a measure of the fiber strain. Then

$$\boldsymbol{\tau} = \frac{\dfrac{\partial \boldsymbol{X}}{\partial s}}{\left|\dfrac{\partial \boldsymbol{X}}{\partial s}\right|} \tag{5}$$

is the unit tangent vector to the fiber. It may be shown (see [8]) that the local force density applied to the fluid is

$$\boldsymbol{f} = \frac{\partial}{\partial s}\left(T\boldsymbol{\tau}\right). \tag{6}$$

Because the force is zero everywhere except on the fiber, $\boldsymbol{F}$ is a distribution, and may be written

$$\boldsymbol{F}(\boldsymbol{x},t) = \int_{\Gamma} \boldsymbol{f}(s,t)\delta(\boldsymbol{x} - \boldsymbol{X}(s,t))ds, \tag{7}$$

where $\delta(\boldsymbol{x})$ is a two-dimensional delta function defined as a product of two Dirac delta functions: $\delta(\boldsymbol{x}) = \delta(x)\delta(y)$. Equations (1)–(7) describe the coupled motion of an elastic fiber interacting with the fluid in which it is immersed, and will be referred to henceforward as the "immersed fiber problem".

3. Linear Stability.

3.1. Problem Reformulation. The presence of a delta-function singularity in the immersed fiber problem, leads us to recast the equations in an alternate form which is more amenable to analysis. In the same spirit as Peskin & Printz [9], we integrate equation (1) across the fiber, assuming the velocity is continuous across Γ, thereby obtaining the following conditions:

$$[\boldsymbol{u}] = 0, \tag{8}$$

$$\nu\boldsymbol{\tau}\cdot[\boldsymbol{n}\cdot\nabla\boldsymbol{u}] = -\frac{\boldsymbol{f}\cdot\boldsymbol{\tau}}{\left|\dfrac{\partial\boldsymbol{X}}{\partial s}\right|}, \tag{9}$$

$$-[p] + \nu\boldsymbol{n}\cdot[\boldsymbol{n}\cdot\nabla\boldsymbol{u}] = -\frac{\boldsymbol{f}\cdot\boldsymbol{n}}{\left|\dfrac{\partial\boldsymbol{X}}{\partial s}\right|}.$$

Here, $[\cdot] = (\cdot)|_{\Omega^+} - (\cdot)|_{\Omega^-}$ denotes the difference in a quantity on either side of the fiber, and $\boldsymbol{n}$ is the unit normal vector to the fiber defined by $\boldsymbol{n}\cdot\boldsymbol{\tau} = 0$. The last jump condition reduces to

$$-[p] = -\frac{\boldsymbol{f}\cdot\boldsymbol{n}}{\left|\dfrac{\partial\boldsymbol{X}}{\partial s}\right|}, \tag{10}$$

upon application of (8) and the incompressibility condition (2). From (9) and (10), it is apparent that both the normal derivative of the velocity and the pressure may be discontinuous across Γ.

Instead of applying equations (1) and (2) on the whole domain Ω, we can avoid the delta-function singularity in the forcing function by solving the Navier-Stokes equations with zero force

$$\boldsymbol{u}_t = -\boldsymbol{u}\cdot\nabla\boldsymbol{u} + \nu\Delta\boldsymbol{u} - \nabla p, \tag{11}$$

$$\nabla\cdot\boldsymbol{u} = 0, \tag{12}$$

separately on the two subdomains Ω^+ and Ω^- of Ω_0 (on each of which the solution is *continuous*), and linking the solutions via the jump conditions (8)–(10). In the resulting problem, (8)–(12), (3)–(6), the singular force has been eliminated in favour of jumps across the fiber.

3.2. Linearized Stability. To determine how a small perturbation in the fiber affects the stability of the flow, consider a small section of the fiber (contained within the subdomain $\Omega_0 \subset \Omega$ depicted in Figure 1) which is approximately horizontal. Suppose that, at equilibrium, the fiber lies along $y = 0$, and is given a small initial perturbation. For the purpose of isolating the influence of the fiber on the flow, let us extend the boundaries of Ω_0 to infinity in the y-direction. This is a reasonable assumption, since we expect that the important dynamics (that is, the dynamics which distinguish fluids with immersed fibers from those without) will occur in the region near the fiber. It also serves to pinpoint modes associated solely with the fiber, since there are no non-trivial discrete modes of Stokes' equations without an immersed fiber on a domain of infinite extent.

A common form of the fiber tension used in immersed boundary computations (for example, in [10] and [9]) is $T = S(|\partial \boldsymbol{X}/\partial s| - 1)$, where S is a constant, corresponding to a fiber which is slack in the reference state, $|\partial \boldsymbol{X}/\partial s| = 1$. In actual computations, however, the fiber is always taken to be under stress, particularly when then system is at equilibrium (*i.e.* when the fluid and fiber are at rest, and the force is zero). Hence, we choose an equilibrium state defined by $|\partial \boldsymbol{X}/\partial s| = \beta > 1$, around which the solution is linearized by supposing a perturbation of the form

$$\boldsymbol{X}(s,t) = (s\beta + \xi(s,t), \eta(s,t)), \tag{13}$$

(refer to Figure 2) and assuming that ξ, η, $\boldsymbol{u}$ and their derivatives are small, at least for some finite time. The linear versions of equations (11) and (12) are simply the

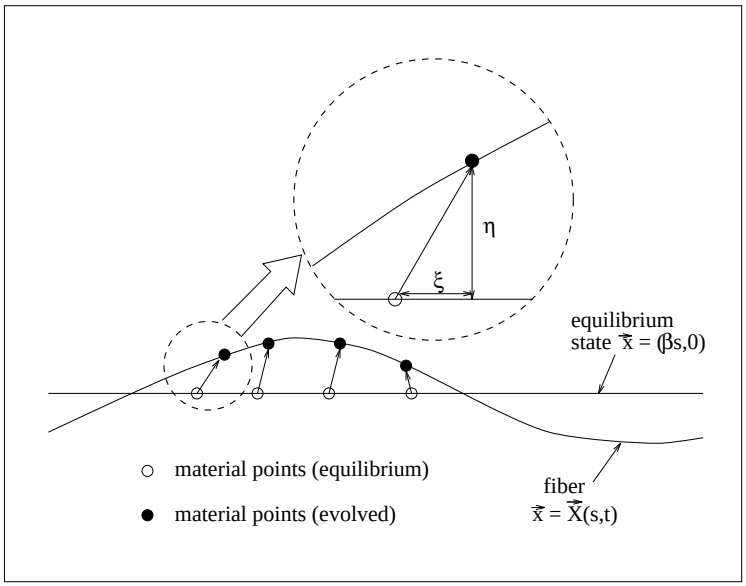

FIG. 2. *Fiber configuration for the 2D model problem.*

Stokes equations

$$\boldsymbol{u}_t = \nu \Delta \boldsymbol{u} - \nabla p, \tag{14}$$

$$\nabla \cdot \boldsymbol{u} = 0, \tag{15}$$

while the fiber evolution equation (3) becomes

$$\frac{\partial \boldsymbol{X}}{\partial t} = \boldsymbol{u}(s, 0, t). \tag{16}$$

Differentiating (13) with respect to s and dropping non-linear terms yields

$$\frac{\partial \boldsymbol{X}}{\partial s} = (\beta + \xi_s\,, \eta_s)\,,$$
$$\left|\frac{\partial \boldsymbol{X}}{\partial s}\right| = \beta + \xi_s\,,$$

which may then be used to obtain the linearized version of (5)

$$\boldsymbol{\tau} = (1, \eta_s/\beta).$$

Expand the tension T from (4) in a Taylor series about the equilibrium state $|\partial \boldsymbol{X}/\partial s| = \beta$ to get

$$T = \sigma_0 + \sigma_1 \xi_s$$

where $\sigma_0 \equiv \sigma(\beta)/\beta$ and $\sigma_1 \equiv \sigma'(\beta)$. As stated earlier, we assume that the fiber is always under tension, and further that the tension is an increasing function of the fiber strain, which for the linear force function amounts to taking $\sigma_0 > 0$ and $\sigma_1 > 0$.

The following physical interpretation may be given to the two tension parameter values:

- σ_0 represents a constant tension in the fiber which (because of its positive sign) acts to restore the fiber to the horizontal whenever any portion is displaced vertically from its equilibrium state. Taking $\sigma_0 = 0$ corresponds to a fiber which is slack in its reference state.
- σ_1 measures the effect that changes in the length of the fiber have on the tension; this parameter is also positive, since stretching ($\xi_s > 0$) or compressing ($\xi_s < 0$) the fiber amounts to increasing or decreasing the tension.

The above expressions for T and τ may be substituted into (6) to obtain the force density

$$\boldsymbol{f} = (\sigma_1 \xi_{ss}\,, \sigma_0 \eta_{ss})\,,$$

from which the following jumps are derived from (8)–(10)

$$[u] = 0, \tag{17}$$
$$[v] = 0, \tag{18}$$
$$\left[\nu \frac{\partial u}{\partial y}\right] = -\sigma_1 \xi_{ss}\,, \tag{19}$$
$$-[p] = -\sigma_0 \eta_{ss}\,. \tag{20}$$

The linearized version of the immersed fiber problem is now given by equations (14)–(20).

It is evident from equation (20) that the pressure may be discontinuous across the fiber. This is of particular concern for the Immersed Boundary Method, which applies a projection scheme over the entire domain, without any special treatment at the discontinuity. Since the projection method assumes a continuous pressure field,

care must be taken to ensure that employing a projection scheme to solve the immersed fiber problem does not introduce any spurious results in numerical computations. On the other hand, the formulation (8)–(12), (3)–(6), in terms of interfacial jumps, should have no such problem since it allows the projection to be applied separately on the two subdomains, each of which has continuous pressure.

In order to isolate the modes associated with the immersed fiber, we look for two separable solutions of the form

$$\begin{Bmatrix} u \\ v \\ p \\ \xi \\ \eta \end{Bmatrix} = e^{\lambda t + i\alpha x} \begin{Bmatrix} \widehat{u}(y) \\ \widehat{v}(y) \\ \widehat{p}(y) \\ \widehat{\xi}_0 \\ \widehat{\eta}_0 \end{Bmatrix}, \tag{21}$$

one on each of the two halves of the domain Ω_0. The wavenumber, α, is real, and we assume, for the moment, that α is positive (we rule out the case of $\alpha = 0$, since this leads simply to the trivial solution). By substituting (21) into (14), forming the linear combination $i\alpha\widehat{u} + d\widehat{v}/dy$, and applying the incompressibility condition (15), we get a second order, linear differential equation for the pressure. After imposing the requirement that the solution be bounded as $y \to \pm\infty$, the solution is determined on either side ("$\pm$") of the fiber to be

$$\widehat{p}^{\pm}(y) = A^{\pm} e^{\mp \alpha y}. \tag{22}$$

We then substitute this expression for the pressure into (14) and (16) to get

$$\widehat{u}^{\pm}(y) = B^{\pm} e^{\mp \mu y} - \frac{i\alpha}{\lambda} A^{\pm} e^{\mp \alpha y} \tag{23}$$

$$\widehat{v}^{\pm}(y) = C^{\pm} e^{\mp \mu y} \pm \frac{\alpha}{\lambda} A^{\pm} e^{\mp \alpha y} \tag{24}$$

$$\widehat{\xi}_0 = \frac{1}{\lambda} B^{+} - \frac{i\alpha}{\lambda^2} A^{+} \tag{25}$$

$$\widehat{\eta}_0 = \frac{1}{\lambda} C^{+} + \frac{\alpha}{\lambda^2} A^{+} \tag{26}$$

where $A^{\pm}$, $B^{\pm}$ and $C^{\pm}$ are constants, and $\mu^2 := \alpha^2 + \frac{\lambda}{\nu}$. Here, we've assumed that $Re(\mu) \geq 0$ (for uniqueness) and that $\mu \neq \alpha$ (*i.e.* $\lambda \neq 0$). Next, we apply the incompressibility condition (15) to the velocities on either side of the fiber, as well as the four jump conditions (17)–(20), which leads to a homogeneous system of six linear equations in the six unknown coefficients. To ensure that there exists a non-trivial solution, we require that the determinant of the system is zero which, after some manipulation, reduces to the following expression

$$(\mu^4 + \alpha\mu^3 - \alpha^2\mu^2 - \alpha^3\mu + \frac{\sigma_0}{2\nu^2}\alpha^3)(\mu^3 + \alpha\mu^2 - \alpha^2\mu - \alpha^3 + \frac{\sigma_1}{2\nu^2}\alpha^2) = 0. \tag{27}$$

In the case when $\lambda = 0$, it may be shown that only the trivial solution satisfies equations (14)–(20) (and hence the requirement that $\mu \neq \alpha$). Recall the earlier assumption that $\alpha > 0$. If we consider the case $\alpha < 0$, the solution for the pressure in (22) is slightly modified, which leads to a dispersion relation identical to (27) except that α is replaced by $-\alpha$. Hence, we may limit our discussion of the stability of the solution to modes with positive wavenumber.

An important consequence of the linearization process is that the modes corresponding to the normal and tangential motion of the fiber are decoupled. Of the two factors in equation (27), the first depends on σ_0 only (which encompasses the normal motion of the fiber), and the other solely on σ_1 (corresponding to a tangential motion). This decoupling is illustrated by the solution plots given in Section 3.3.4.

3.3. Results. To simplify the analysis in this section, we recast the problem in terms of the following dimensionless variables:

$$\widetilde{\mu} = \mu / \left(\frac{\sigma_1}{\nu^2}\right), \quad \widetilde{\alpha} = \alpha / \left(\frac{\sigma_1}{\nu^2}\right) \quad \widetilde{\lambda} = \lambda / \left(\frac{\sigma_1^2}{\nu^3}\right), \quad \text{and} \quad \gamma = \frac{\sigma_0}{\sigma_1}. \tag{28}$$

The dispersion relation (27) may now be written

$$(\widetilde{\mu}^4 + \widetilde{\alpha}\,\widetilde{\mu}^3 - \widetilde{\alpha}^2\widetilde{\mu}^2 - \widetilde{\alpha}^3\widetilde{\mu} + \frac{\gamma}{2}\widetilde{\alpha}^3)(\widetilde{\mu}^3 + \widetilde{\alpha}\widetilde{\mu}^2 - \widetilde{\alpha}^2\widetilde{\mu} - \widetilde{\alpha}^3 + \frac{1}{2}\widetilde{\alpha}^2) = 0, \tag{29}$$

where $\widetilde{\lambda} = \widetilde{\mu}^2 - \widetilde{\alpha}^2$.

Since (29) is a polynomial equation in $\widetilde{\mu}$ with factors of degree 3 and 4, analytic expressions for the roots are easily derived using the symbolic algebra package Maple [3]. A contour plot of the largest growth rate, $Re(\widetilde{\lambda})$, is given in Figure 3 for a range of $\widetilde{\alpha}$ and γ, with the region of stability (where $Re(\widetilde{\lambda}) < 0$) denoted by dashed lines. It is not surprising that this is precisely the region where $\gamma > 0$ (*i.e.* $\sigma_0 > 0$ and $\sigma_1 > 0$); that is, the fiber modes are stable when the tension force acts to oppose any stretching or curvature of the fiber.

Unfortunately, the foregoing discussion does not allow us to conclude that the immersed fiber problem is stable. By extending Ω_0 to infinity in the y-direction, we picked out the modes arising solely from the presence of the fiber, and so demonstrated that these interfacial modes decay in time. To draw conclusions about the stability of the full spectrum requires an analysis of the doubly-periodic domain (for which the Stokes equations without an immersed fiber exhibit modes with a growth rate $\lambda = -\nu\alpha^2$, α an integer). The dispersion relation for the periodic case is not a polynomial, but rather a transcendental equation, from which it is difficult, if not impossible, to obtain all modes.

Nevertheless, we can still glean some useful information from the previous analysis of the immersed fiber problem. Now that the modes associated with the fiber are known to be linearly stable, we'd like to attack the question: "How rapidly does a perturbation in the fiber die out in time?" To simplify our investigation of the solution modes, it is appropriate to consider three cases: namely that of small, intermediate and large values of the non-dimensionalized wavenumber, $\widetilde{\alpha}$. The small $\widetilde{\alpha}$ case is the one we are really interested in (since Peskin's numerical examples fall into this regime), and the other two cases are included for completeness.

3.3.1. Small wavenumber. Equation (29) was solved for $\gamma = 2$, and all "physical" roots (*i.e.* roots for which $Re(\widetilde{\mu}) > 0$) were plotted in Figure 4 for values of $\widetilde{\alpha} \in [0, 0.5]$. An explicit form for the dependence of the growth rate on the wavenumber may be determined by computing a regular asymptotic expansion for each root in powers of the non-dimensionalized wavenumber $\widetilde{\alpha}$, as $\widetilde{\alpha} \to 0$. There are, in fact,

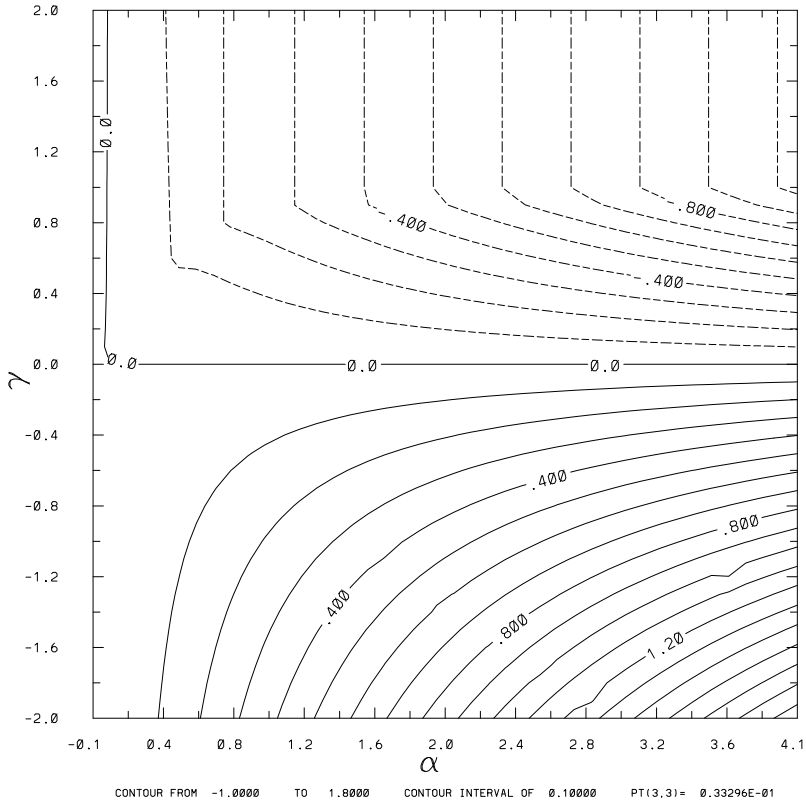

FIG. 3. *Contours of the maximum scaled growth rate* $Re(\widetilde{\lambda})$ *plotted versus* $\gamma = \frac{\sigma_0}{\sigma_1}$ *and scaled wavenumber* $\widetilde{\alpha}$. *The stable region is marked by dashed contours and lies above and to the right of the 0.0 contour.*

two complex conjugate pairs of roots, given in terms of dimensional variables as

$$\lambda_0^{+} \sim i\nu \left(\frac{\sigma_0}{2\nu^2}\right)^{\frac{1}{2}} \alpha^{\frac{3}{2}} - \frac{\nu(1+i)}{2\sqrt{2}} \left(\frac{\sigma_0}{2\nu^2}\right)^{\frac{1}{4}} \alpha^{\frac{7}{4}} - \frac{\nu}{4}\alpha^2 + \mathcal{O}(\widetilde{\alpha}^{\frac{9}{4}}),$$

$$\lambda_0^{\triangle} \sim -i\nu \left(\frac{\sigma_0}{2\nu^2}\right)^{\frac{1}{2}} \alpha^{\frac{3}{2}} - \frac{\nu(1-i)}{2\sqrt{2}} \left(\frac{\sigma_0}{2\nu^2}\right)^{\frac{1}{4}} \alpha^{\frac{7}{4}} - \frac{\nu}{4}\alpha^2 + \mathcal{O}(\widetilde{\alpha}^{\frac{9}{4}}),$$

$$\lambda_0^{\times} \sim -\frac{\nu(1-i\sqrt{3})}{2} \left(\frac{\sigma_1}{2\nu^2}\right)^{\frac{2}{3}} \alpha^{\frac{4}{3}} - \frac{\nu(1+i)}{\sqrt{3}} \left(\frac{\sigma_1}{2\nu^2}\right)^{\frac{1}{3}} \alpha^{\frac{5}{3}} + \mathcal{O}(\widetilde{\alpha}^{\frac{7}{3}}),$$

$$\lambda_0^{\square} \sim -\frac{\nu(1+i\sqrt{3})}{2} \left(\frac{\sigma_1}{2\nu^2}\right)^{\frac{2}{3}} \alpha^{\frac{4}{3}} - \frac{\nu(1-i)}{\sqrt{3}} \left(\frac{\sigma_1}{2\nu^2}\right)^{\frac{1}{3}} \alpha^{\frac{5}{3}} + \mathcal{O}(\widetilde{\alpha}^{\frac{7}{3}}),$$

which substantiates the results in Figure 4. Note that beyond a value of $\widetilde{\alpha} \approx 0.4$, two of the roots merge and split into a pair of real roots, and shortly thereafter (at $\alpha \approx 0.5$), one of those roots ($\lambda^{\times}$) becomes non-physical (*i.e.* $Re(\mu)$ becomes negative).

The asymptotic expressions given above may be used to relate the linear stability of the immersed fiber problem to the stiffness of an associated numerical scheme such as the Immersed Boundary Method. A typical computation, such as that in [6], is on a domain $\Omega = [0,1]^2$, with a grid spacing of $\Delta x = \Delta y = 1/64$ (all measurements being

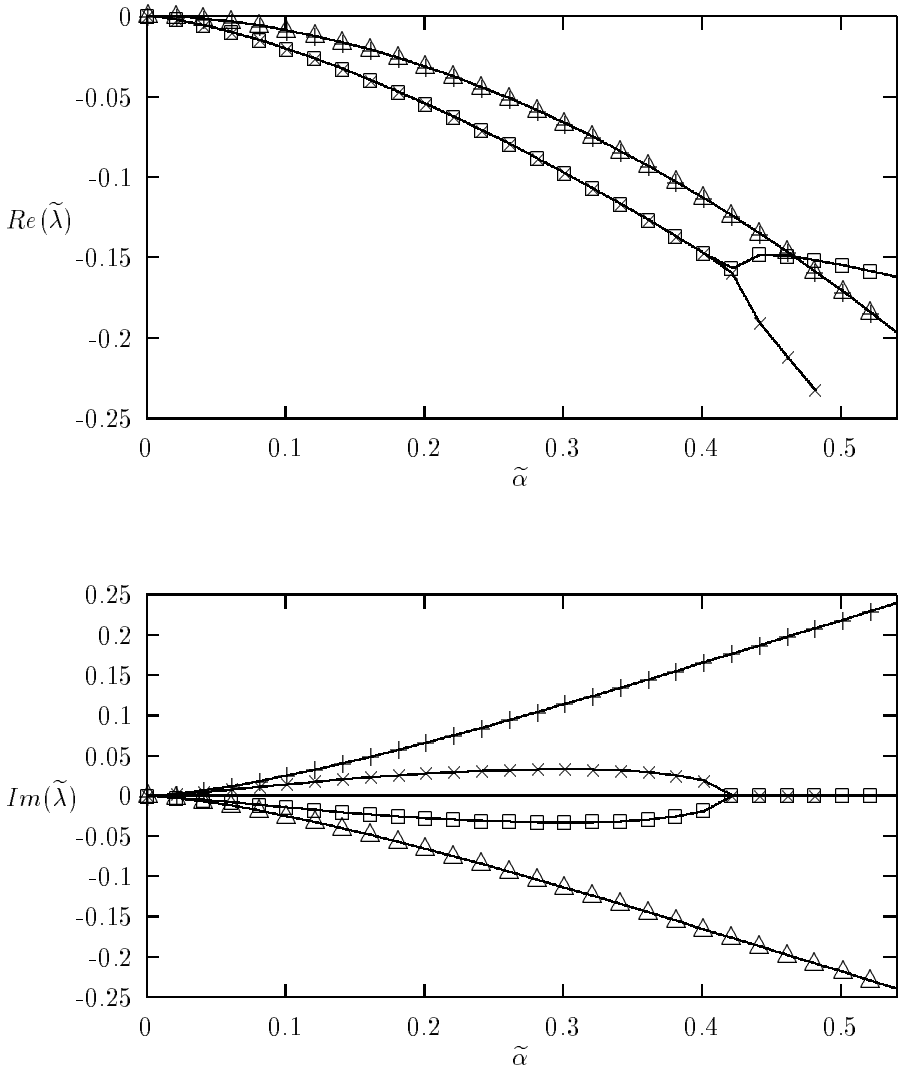

FIG. 4. *Plots of the real and imaginary part of the scaled growth rate* $\widetilde{\lambda}$ *versus wavenumber* $\widetilde{\alpha}$ *for each of the physical roots, denoted by* $+$, $\triangle$, $\square$ *and* $\times$. *The value of* γ *is taken to be 2.*

in cm). This discretization allows the computation to resolve modes with a maximum wavenumber of $\alpha_{max} = 1/\Delta x = 64$. We can assess the stiffness of the method by considering the growth of modes with wavenumbers restricted to the range $\alpha \in [0, 64]$.

As mentioned earlier, it is the small wavenumber regime which is of most interest, because this is where Peskin's computations are found to lie. Based on the information in [6], we take the parameters to be $\nu = 0.01\ cm/s^2$ and $\sigma_0 = \sigma_1 = 10,000\ cm^3/s^2$ (*i.e.* $\gamma = 1$). For $\alpha \in [0, 64]$, the non-dimensionalized wavenumber lies in the range $\widetilde{\alpha} \in [0, 6.4 \times 10^{-5}]$, which clearly indicates that Peskin's numerical examples lie in the small wavenumber region. It may not be appropriate to take the maximum α to be

as large as 64, since the approximation to the delta-function used in the Immersed Boundary Method may serve to lower the effective wavenumber in computations. However, we will use this value to illustrate the stiffness in the problem, which is present even for smaller α.

In the course of his immersed boundary computations, Peskin has observed that a very small time step is required in order to achieve stability. This seems to suggest that the problem is stiff, and we'd like to find an explanation for this stiffness in terms of the analytical results above. Examining the asymptotic expressions for the growth rates, we find that the highest wavenumber ($\alpha = 64$) leads to $Re(\lambda^+) = Re(\lambda^{\triangle}) \approx -4.4\times 10^2$ and $Re(\lambda^{\times}) = Re(\lambda^{\square}) \approx -1.8 \times 10^5$. Hence, the fiber modes have eigenvalues with $Re(\lambda) \in [-1.8\times 10^5, 0]$, which can be compared to the modes of Stokes equations with $\lambda^S = -\nu\alpha^2 \in [-4.1 \times 10^1, 0]$. By observing the wide disparity in growth rates, it is clear that the immersed fiber problem is stiff and, in fact, the stiffness is much more severe than that present in a Stokes flow without immersed fibers. This deterioration in conditioning of the problem is due to the modes which arise from the interaction of the fiber with the fluid, through the combination of large fiber tension parameters, σ_0 and/or σ_1, and small viscosity.

In terms of numerical computations, the presence of stiff modes suggests the use of an implicit time-stepping scheme. The analytical justification given here backs up the conclusion of Tu & Peskin in [10] that by applying a fully implicit scheme, a considerable improvement in numerical stability can be realized. They also observe that "in its present form, the fully implicit scheme is probably too expensive for practical application"[10, p. 1376], and suggest that a more efficient implementation be developed. It is our hope that the analysis given here may help in devising a more efficient scheme, by allowing the stiff interface modes to be singled out.

3.3.2. Intermediate wavenumber. Figure 5 contains a plot of the scaled growth rate $\widetilde{\lambda}$ for values of $\widetilde{\alpha}$ in the intermediate range $[0, 2]$. It is evident that, in addition to the bifurcation at $\widetilde{\alpha} \approx 0.4$, mentioned in the previous section, there is a similar point at $\widetilde{\alpha} \approx 1.7$, at which a complex conjugate pair merges and splits into two real roots.

3.3.3. Large wavenumber. Figure 6 depicts $\widetilde{\lambda}$ for $\widetilde{\alpha} \in [0, 5]$. To determine the dependence of λ on α for large α, we again perform an asymptotic expansion of the roots as $\widetilde{\alpha} \to \infty$ to obtain the following three real roots (in terms of dimensional variables):

$$\begin{aligned}
\lambda_\infty^{\square} &\sim -\frac{\sigma_1}{4\nu}\alpha - \frac{\sigma_1^2}{64\nu^3} - \frac{3\sigma_1^3}{1024\nu^5}\alpha^{-1} + \mathcal{O}(\widetilde{\alpha}^{-2}),\\
\lambda_\infty^{\triangle} &\sim -\frac{\sigma_0}{4\nu}\alpha - \frac{3\sigma_0^2}{64\nu^3} - \frac{19\sigma_0^3}{1024\nu^5}\alpha^{-1} + \mathcal{O}(\widetilde{\alpha}^{-2}),\\
\lambda_\infty^{+} &\sim -\nu\alpha^2 + \frac{\sigma_0^2}{4\nu^3} - \frac{\sigma_0^3}{4\nu^5}\alpha^{-1} + \mathcal{O}(\widetilde{\alpha}^{-2}).
\end{aligned}$$

It is clear that $\lambda_\infty^{\square}$ and $\lambda_\infty^{\triangle}$ grow linearly in α to first order, while the expansion for λ_∞^{+} certifies that the third mode varies quadratically with the wavenumber, which is suggested by the shape of the curves in Figure 6. Like solutions to Stokes' equations without an immersed fiber, the mode represented by λ_∞^{+} gives rise to stiffness in the problem, for as the wavenumber varies, the growth rates take on widely disparate values. However, the presence of a fiber gives rise to an additional source of stiffness in $\lambda_\infty^{\square}$ and $\lambda_\infty^{\triangle}$. For these two modes, λ may be large even for moderate values of α if the viscosity is small or the tension parameters σ_1 or σ_0 are large. However, when

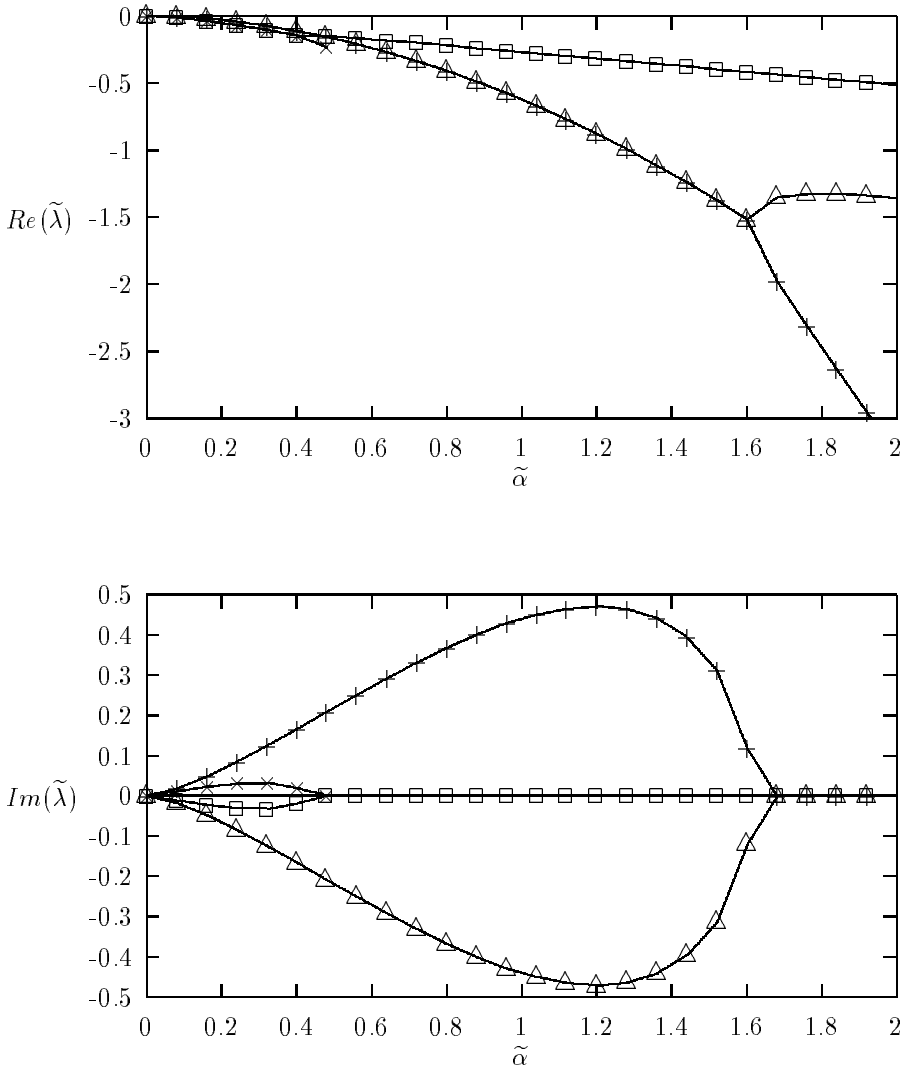

FIG. 5. *Plots of the real and imaginary parts of the scaled growth rate versus wavenumber for each of the physical roots , denoted by* $+$, $\times$, $\Box$ *and* $\triangle$. *In this plot, it is clear that there are two bifurcation points, at values of approximately 0.4 and 1.7, where two complex conjugate roots merge and split into two real roots.*

α is taken large enough (*i.e.* when the solution is resolved to a fine enough level), the Stokes-like mode (λ_{∞}^{+}) is the dominant one.

3.3.4. Solution plots. Figure 7 gives a pictorial representation of the the modes found by substituting the values for λ and μ into the solutions from (22)–(26), with parameter values $\nu = 1$, $\sigma_0 = 1$, $\sigma_1 = 1$, $\alpha = 1$ and $t = 0$. There are only three "real" modes satisfying the condition $Re(\mu) \geq 0$. The plots for $\lambda^{\Box}$ correspond to the mode which arises from the factor in (27) involving σ_1, and thus embody the

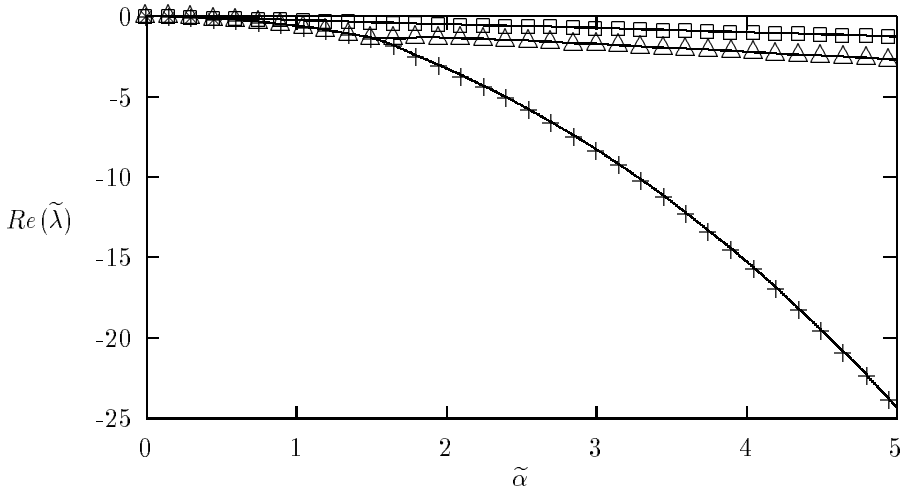

FIG. 6. *Plot of the nondimensionalized growth rate* $Re(\widetilde{\lambda})$ *versus* $\widetilde{\alpha}$ *for each of the three roots satisfying* $Re(\mu) > 0$. *The value of* γ *is taken here to be* 2. *The imaginary part of the roots is zero for all values of scaled* $\widetilde{\alpha} > 1.7$.

horizontal expansion and contraction of the fiber (which is obvious from the velocity vector plot). The normal velocity and pressure for $\lambda^{\square}$ are smooth, while the tangential velocity is not; hence, the fiber force for this mode arises solely from the first jump condition (19). On the other hand, the remaining two modes, $\lambda^{\triangle}$ and λ^{+}, comprise the normal (vertical) motion of the fiber. The source of this motion is the constant tension, σ_0, which acts normal to the fiber, and arises from the second jump condition (20). The modes in this case have a smooth velocity and discontinuous pressure.

4. Summary and Conclusions. Eliminating the delta-function in favour of jump conditions in the immersed fiber problem allows us to split the problem into two continuous ones, which are more amenable to analysis. The linearized problem yields interesting observations regarding the behaviour of solutions which give insight into flows in the presence of immersed fibers. Furthermore, the dependence of the modes on the wavenumber helps guide us in selecting an appropriate numerical scheme.

It is clear from the jump condition (10) that the pressure is discontinuous. A projection method which is based on the "jump" formulation has the advantage that the projection step will not be applied across the fiber, but only on subdomains where the pressure is continuous. It is unclear what effect the discontinuity will have on the projection step in the Immersed Boundary Method, and so this question deserves further investigation.

After examining the dependence of the growth rate on values of the parameters which define the linearized fiber tension, it is evident that the solutions modes arising solely from the interaction of an immersed fiber with the surrounding fluid are stable for precisely those tension forces which are physically reasonable. That is, instability occurs only for the non-physical case where contraction or expansion of the fiber is accompanied by "positive feedback".

By solving for the roots of the modal equation numerically, we discovered that

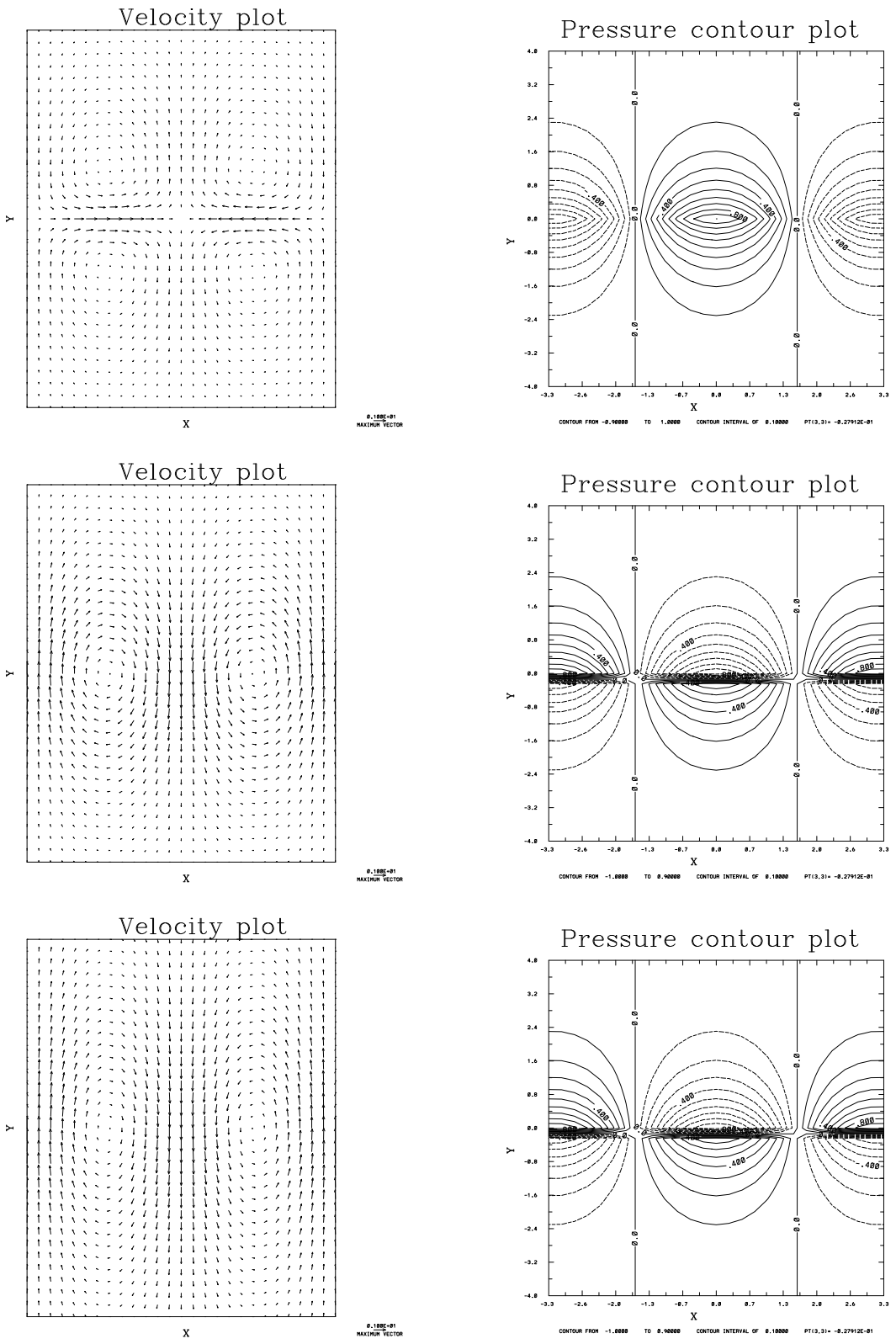

FIG. 7. *Velocity vector plots and pressure contours for the modes* $\lambda^{\square}$ *(top),* $\lambda^{\triangle}$ *(middle) and* λ^{+} *(bottom). Parameter values:* $\nu = 1$, $\sigma_0 = 1$, $\sigma_1 = 1$, $\alpha = 1$, $t = 0$.

the growth rates of the solution modes vary to a wide degree, and hence the problem is stiff. Furthermore, the main source of stiffness is not the modes arising from the Stokes flow, but rather those originating from the interaction of the fluid with the fiber. We conclude that a numerical scheme will have to employ implicit time-stepping of some type in order to devise an efficient scheme. Tu & Peskin made the same conclusion based on numerical evidence, but also found that the use of a fully implicit scheme is impractical. Asymptotic expansions of the roots for both large and small wavenumbers are used to back up the observations, and give an explicit form for the dependence of the growth rate on the parameters in the problem. This verifies that the presence of the fiber has a significant effect on the flow, which is of particular importance in computations.

Notwithstanding the stiffness arising from the interfacial modes, there is still hope for improving the conditioning of the Immersed Boundary Method by singling out the problem modes. In particular, it may be possible to derive a semi-implicit scheme which handles the stiff interfacial modes in a special way, without requiring the expensive step to a fully implicit solver.

Acknowledgements. We would like to thank Randall LeVeque and Charles Peskin for their helpful comments.

REFERENCES

[1] R. P. Beyer and R. J. LeVeque, *Analysis of a one-dimensional model for the immersed boundary method*, SIAM J. Num. Anal., 29 (1992), pp. 332–364.

[2] R. P. Beyer, Jr., *A computational model of the cochlea using the immersed boundary method*, J. Comp. Phys., 98 (1992), pp. 145–162.

[3] B. W. Char et al., *Maple V Language Reference Manual*, Springer-Verlag, 1991.

[4] L. J. Fauci and C. S. Peskin, *A computational model of aquatic animal locomotion*, J. Comp. Phys., 77 (1988), pp. 85–108.

[5] R. J. LeVeque and Z. Li, *The immersed interface method for elliptic equations with discontinuous coefficients and singular sources*, SIAM J. Num. Anal., 31 (1994).

[6] A. A. Mayo and C. S. Peskin, *An implicit numerical method for fluid dynamics problems with immersed elastic boundaries*, in Fluid Dynamics in Biology: Proceedings of the AMS–IMS–SIAM Joint Summer Research Conference on Biofluiddynamics (Contemporary Mathematics, vol. 141), A. Y. Cheer and C. P. van Dam, eds., American Mathematical Society, 1993, pp. 261–277.

[7] C. S. Peskin, *Numerical analysis of blood flow in the heart*, J. Comp. Phys., 25 (1977), pp. 220–252.

[8] C. S. Peskin and D. M. McQueen, *A three-dimensional computational model for blood flow in the heart I. Immersed elastic fibers in a viscous incompressible fluid*, J. Comp. Phys., 81 (1989), pp. 372–405.

[9] C. S. Peskin and B. F. Printz, *Improved volume conservation in the computation of flows with immersed elastic boundaries*, J. Comp. Phys., 105 (1993), pp. 33–46.

[10] C. Tu and C. S. Peskin, *Stability and instability in the computation of flows with moving immersed boundaries: A comparison of three methods*, SIAM J. Sci. Stat. Comp., 13 (1992), pp. 1361–1376.